Chapter VIII

Homology modeling and MD simulation of the Cytolethal distending toxin B gene of Helicobacter hepaticus ATCC 51449

8.1: Introduction

H. hepaticus is a naturally occurring pathogen of mice, has been used as a model for the study of hepatic carcinogenesis and gastrointestinal disease. *H. hepaticus* produces a soluble toxin known as cytolethal distending toxin (Cdt). Cdt is a bacterial toxin that induces cell cycle arrest of cultured cells in the G2 phase. It has been found in a number of mucosal pathogens, including *Campylobacter jejuni* (Johnson & Lior 1988) and other *Campylobacter* species (Pickett *et al.,* 1996), certain *Escherichia coli* strains (Bouzari & Varghese 1990; Johnson & Lior 1988b) *Shigella dysenteriae* (Okuda *et al.,* 1995), *Haemophilus ducreyi* (Cope *et al.,* 1997) and *A. actinomycetemcomitans* (Sugai *et al.,* 1998) and *H. hepaticus* (Young *et al.,* 2000). Cdt is composed of three subunits, CdtA, CdtB and CdtC, which form a tripartite complex (Saiki *et al.,* 2001; Saiki *et al.,* 2004; Lara-Tejero & Gala'n 2002). CdtA and CdtC are required for the delivery of CdtB, the active subunit (Lara-Tejero & Gala'n 2001; Deng & Hansen 2003; Lee *et al.,* 2003; Shenker *et al.,* 2004). On delivery into host cells by CdtA and CdtC, the active subunit CdtB is transported to the nucleus and causes DNA damage (Elwell & Dreyfus 2000; Lara-Tejero & Gala'n 2000). CdtB has an amino acid sequence similar to the DNase I family of proteins. The CdtB gene is found to be the most conserved among the three Cdt genes (Pickett et al., 1996; Young *et al.,* 2000; Mayer *et al.,* 1999). Little work has been carried out on the CDT of *H. hepaticus*, owing to a limited toxin production by the bacterium and to the difficulties in producing a recombinant toxin. It makes it difficult to produce the toxin in sufficient quantities to perform cell culture studies (Avenaud *et al.,* 2004).Studies with CDT of *Campylobacter jejuni* and *E. coli* have shown that CdtB has a DNase activity in vitro and suggested that CdtB could be the active subunit of the holotoxin (Lara-Tejero & Galan 2000; Elwell & Dreyfus 2000; Elwell *et al.,* 2001). Indeed, mutations in the CdtB's DNase

catalytic site abolish the cellular toxic activity of the holotoxin (Lara-Tejero & Galan 2000; Elwell & Dreyfus 2000). As CdtB DNase activity is very poor in vitro (Lara-Tejero & Galan 2000) some authors suggested that CdtB could be a phosphatase for either Wee1 kinase or CDC25 phosphatase, or for other cell cycle regulatory proteins (Pickett & Whitehouse 1999; Dlakic 2000; Dlakic 2001).

Cdt induces DNA double strand breaks in target cells. This was shown in yeast cells transfected with the CdtB gene (Hassane *et al.,* 2001) and in mammalian cells naturally intoxicated by extracellular treatment with the toxin (Frisan *et al.,* 2003). The subcellular target of Cdt is known to be DNA. In *H. hepaticus* ATCC51449, four conserved residues (S93, R139, N190 and T224) are present (Dassanayake *et al.,* 2005).

It is observed that the CdtB does indeed possess a DNase activity, which is absent in the CdtA and CdtC subunits, and that this activity can be abolished by an amino acid change in the region identified as potentially responsible for this activity. Three CdtB mutants of *H. hepaticus* were constructed by Avenaud *et al,* one of them in the potential DNase activity region (CdtBH265L mutant) and two others in the potential phosphatase activity region (CdtBN27I and CdtBE60V mutants) (Avenaud *et al.,* 2004). N27 residue was noted to be important as it surrounds the catalytic pocket and possibly the phosphate (Dlakic 2000). It is now widely documented in several bacteria that CdtB is responsible for the cell toxicity of the CDT via its DNase activity (Lara-Tejero & Galan 2002).

H. hepaticus ATCC51449 was isolated from liver tissue in the course of the initial investigation of the outbreak of hepatitis (Ward *et al.,* 1994). In spite of increasing research effort and complete genome of the bacteria *H. hepaticus* ATCC51449 is sequenced (Suerbaum *et al.,* 2003) but the structure of Cdt of *H. hepticus* is not solved yet.

The aim of this work is to construct the 3D model of CdtB proteins from *H. hepaticus* ATCC51449 strains taking the crystal structure of Cytolethal distending toxin B (CdtB) of

A. actinomycetemcomitans (Yamada *et al.,* 2006) as template and to perform molecular dynamics simulation and principal component analysis to understand its motional properties and conformational space traversed by it.

8.2: Materials and methods

The amino acid sequences of the Cytolethal distending toxin B gene (CdtB) of *H. hepaticus* ATCC 51449 bearing protein id NP_860978.1 was obtained from the IMG database (www.img.jgi.doe.gov) (Suerbaum *et al.,* 2003).The protein is 273 amino acid length and it was confirmed that the 3D structure of the protein was not available in Protein Data Bank (http://www.rcsb.org/pdb/home/home.do), consequently the current work of constructing the 3D model of the CdtB gene of *H. hepaticus* ATCC 51449 strains was initiated.

Homology modeling

The preliminary task in the homology modeling technique is to recognize protein structures linked to the target sequence and subsequently select those that will be used as templates (Centeno et al., 2005). PSI-BLAST (Altschul et al., 1997) was carried out against database specification of PDB proteins, which were available at the National Centre for Biotechnology Information (NCBI) Web server (http://www.ncbi.nlm.nih.gov/blast/) to find out remote similarities. We retrieved the known homologous structures of CdtB of *H. hepaticus* ATCC 51449 from the protein data Bank (PDB). We found that protein Cdt from *A. actinomycetemcomitans* [PDB entry: 2F2F (Chain B)] was structural template (percentage sequence identity 47.12) (See Fig. 1).

An optimal alignment between the target sequence and template is required to construct a 3D model of the target protein, after the template sequence has been recognized. Multiple sequence alignments were performed using ClustalW 1.83 using default settings and the aligned sequences were extracted in (.) PIR format (Thompson *et al.,* 1994). The aligned sequences were converted into (.) ALI format (Sali & Blundell 1993) the acquired alignments

were crucially assessed in terms of number, length and position of the gaps to make it more reliable.

CLUSTAL W (1.81) multiple sequence alignment of the templete sequence and the cdtB gene from from *Helicobacter hepaticus* ATCC 51449 (Protein id NP_860978.1)

```
NP_860978.1     MRILLCFLMSFTFALANLEDYRVSTWNLQGSSANTESKWNISVRQLITGDNPANILMVQE
2F2F            ----------------NLSDFKVATWNLQGSSAVNESKWNINVRQLLSGEQGADILMVQE
                              **.*:.*:*******  .******.****:.*:: *:******

NP_860978.1     AGAIPASARRTGRMVQPGGTPVEEFTWELGTYSRPNTVYIYYAPLDVGARRVNLAIVSDR
2F2F            AGSLPSSAVRTSRVIQHGGTPIEEYTWNLGTRSRPNMVYIYYSRLDVGANRVNLAIVSRR
                **:.*:** **.*::* ****:**:**:*** **** *****: *****.******** *

NP_860978.1     RADEVLVVHQNVVATEASRPAIGIRIGNDVFFNIHALASGGGDAPALVTAVHDNFINMP-
2F2F            QADEAFIVHSDSSVLQS-RPAVGIRIGTDVFFTVHALATGGSDAVSLIRNIFTTFTSSPS
                :***.::**.:  . :: ***:*****.****.:****:**.** :*:  :. .* . *

NP_860978.1     -----QINWLIAGDFNRDPALLQSGLDTR--IANHIRITAPNSATHFSSRGTNRTLDYAV
2F2F            SPERRGYSWMVVGDFNRAPVNLEAALRQEPAVSENTIIIAPTEPTHRSG----NILDYAI
                       .*::.***** *. *::.*  .  ::::  * **...** *.    . ****:

NP_860978.1     VGRSSPSRSTIVLPQIAAILMAANIRAHLSSDHSPVHFGRF-
2F2F            LHDAHLPRREQARERIGASLMLNQLRSQITSDHFPVSFVHDR
                :  :  .*   .  :*.* **  ::*:::;*** ** * :
```

Figure-1: **Alignment:** Alignment of target protein (2F2F) and cytolethal distending toxin protein B (CdtB) from *H. hepaticus* ATCC51449.

The initial 3D model of the CdtB gene of *H. hepaticus* ATCC 51449 was constructed by MODELLER 9v4 program (Sali & Blundell 1993) using the alignment between the CdtB gene of *H. hepaticus* ATCC 51449 and the template protein(2F2F chain B).

Model evaluation:

VERIFY3D was used to validate the refined structures. For evaluation of their internal quality and reliability, the refined model was subjected to the following tests: ProSA (Wiederstein & Sippl 2007) analysis was performed to assess the accuracy and reliability of the modelled structure and check the 3D model for potential errors. Here, the 3D structure of the protein model is compared to its own amino-acid sequence taking into consideration a 3D profile calculated from the atomic coordinates of the structure of correct protein (Eisenberg *et al.,*

1997). Presence of pockets in the structure was predicted using CASTp server (Dundas et al 2006). The refined model was submitted to ProFunc (http://www.ebi.ac.uk/thronton-srv/databases/ProFunc) (Laskowski *et al.,* 2005) to recognize the functional region in the protein. The program PROCHECK (Laskowski *et al.,* 1993) has performed assessment of the predicted model of the CdtB of *H. hepaticus* ATCC 51449 to evaluate their backbone conformation using a Ramachandran plot (Ramachandran *et al.,* 1963). Molecular surface and electrostatic potential of modelled CdtB subunit from *H. hepaticus* ATCC 51449 were predicted using AutoDock Tools version 1.5.2 revision 2 (Goodshell *et al.* 1996).

Molecular dynamics simulation

An understanding of the structural dynamics of the protein is essential to gain greater insights into their important biological functions (Yang *et al.,* 2006). The studies on the structural dynamics were performed using the GROMACS. Taking the rough 3D model of the Cytolethal distending toxin B gene was constructed by MODELLER 9v4 program was used as starting structures for dynamics of the protein model. A single monomer was solvated with SPC water molecules in a cubic box having edge length of 40A. The simulation was performed using GROMACS (Lindahl *et al.,* 2001). The LINCS algorithm was used to constrain all bond lengths (Hess *et al.*, 1997). A cutoff of 0.9 nm for Lennard-Jones interactions was used and the particle mesh Ewald method (Darden et al., 1993; Essmann *et al.,* 1995) was employed to calculate longer-range electrostatic contributions on a grid with 0.12-nm spacing and a cutoff of 1.0 nm. The simulation was conducted at constant temperature (300 K), coupling each component separately to a temperature bath using the Berendsen coupling method (Berendsen et al., 1984). The time step was 2 fs, with coordinates stored after every 4 ps. MD simulation was performed for six nano seconds. Before running simulation, an energy minimization was performed in steepest descent method (converged at 107 steps) and this was followed by 1.0ns of simulation imposing

positional restraints on the non-H atoms. The positional restraints were then released and 6 ns production run were obtained and analyzed. Analysis programs from GROMACS were used.

Principal component analysis

Principal component analysis (PCA) (Amadei et al., 1993; Garcia 1992; Das & Mukhopadhyay 2007) was performed with the MD trajectory.

8.3: Results

Homology modeling and Model evaluation:

The target sequence [cytolethal distending toxin protein B(CdtB) of *H. hepaticus* ATCC 51449] compared with more identity and releated family using BLAST search and the best template was found 2F2F2 [PDB ID] chain B, which is a crystal structure cytolethal distending toxin protein B(CdtB) of *A. Actinomycetemcomitans*. The B chains of this protein (2F2F2) revealed percent sequence identity 48.71 with target sequence (Fig. 1).

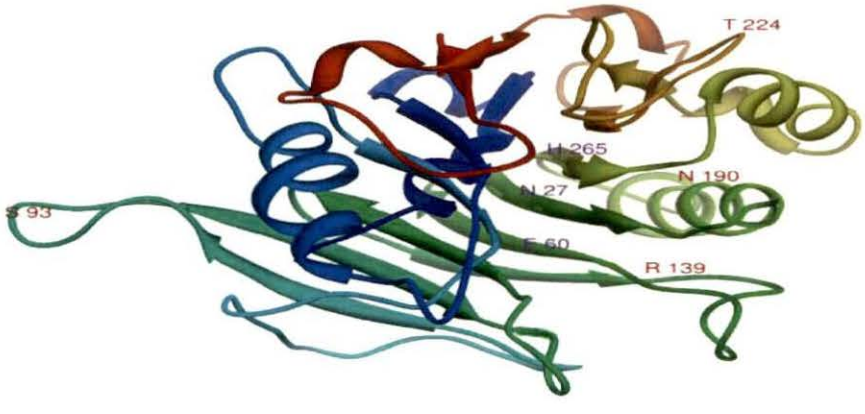

Figure-2: **Ribbon diagram:** The ribbon diagram of the modelled CbtB protein from *H. hepaticus* ATCC51449 is depicted and the four DNA binding residues, namely S93, R139, N190, and T224 are labelled with red colour and the DNase activity region i.e. N27, E60, and H265 are labeled with pink colour.

The modelled structure of the CdtB protein from *H. hepaticus* ATCC51449 is presented in Fig. 2. Four DNA binding residues, namely S93, R139, N190, and T224 are labelled with red colour and the DNase activity region i.e. N27, E60, and H265 are labeled with pink colour in the ribbon diagram of the modelled CbtB protein from *H. hepaticus* ATCC51449 and is also presented in Fig. 2.

Some of the important features of the modelled protein are summarized in Table 1.

Table 1: Summary of the characteristics of the cytolethal distending toxin protein B from *Helicobacter hepaticus* ATCC

General characteristics	CdtB	Characteristics of secondary structure	CdtB
Molecular weight	29,812.8	Alpha helix	20.88%
Net Partial Charge	3.00005	Extended strand	30.77%
Number of atoms	2687	Random coil	48.35%

Figure-3: **Pockets for ligands interaction:** Total of 33 pockets for ligands interaction region in the CdtB protein from *H. hepaticus* ATCC51449 are predicted using CASTp servers and visualization on SPDBV software.

CASTp program (Dundas *et al.,* 2006) demonstrated the presence of a total of 33 pockets for ligands interaction in the CdtB protein with varying area and volume (see Table-2).

Table-2: Total of 33 pockets for ligands interaction region in the Cdtb protein from *Helicobacter hepaticus* ATCC51449 is predicted using CASTp server.

Pocket No.	Residue No.	Area	Volume
1	ARG139,PRO140,ILE154,HIS155	24.9	11.6
2	ILE154,ILE167,ILE185	25.5	11.9
3	ARG69,GLU88	0.8	1.7
4	ILE154,ALA164, ILE185,PHE189	25.8	12.2
5	GLY160, ARG191,LEU195,ARG226	24.4	13.7
6	PHE219,HIS260	0.6	1.5
7	ILE41,SER42,ALA259,HIS260	28.4	13.9
8	ALA141,PHE152,ASN153,ILE154,ILE185	29.3	14.6
9	HIS207,ARG235,PRO238,SER239,ILE243	37.1	20.2
10	ALA141,ILE154,LEU167,ILE185	27.4	13.2
11.	THR35,GLU36,ALA63,ILE64,PRO65	26.6	13.2
12	THR25,TRP26,ASP229,SER266	42	23.1
13	ALA254,ILE257,LEU262,SER266,PRO267	35.9	19.6
14.	SER42,GLN45,ILE257,ALA259,HIS260,LEU261	56.1	33.9
15	PHE13,GLU19,TRY21,ILE248,GLY271,ARG272	38	21.4
16.	ARG44,ILE47,THR48,LEU89	21.7	15.8
17	SER138,ARG139,HIS155,LEU157,ASP163	41	20.2
18	GLN197,ILE208,ARG209,ILE210,ILE243,VAL244	39.5	22.3
19	THR169,HIS172,ARG203,ILE204	23.6	14
20	ALA164,VAL168,ILE185,PHE189,LEU196,VAL232	55.6	30.8
21	PRO165,VAL168,GLY199,LEU200,THR202,ARG203,ILE204	64.2	52.3
22	GLU19,ASP20,TYR21,ARG22,GLY271,ARG272	40.3	30.1
23	ASN51,ILE251,LEU252,MET253,ALA255,ASN256,HIS269	50.4	47.1
24	SER67,ARG69,THR86,TRP87,GLU88	64.1	51.3
25	GLU60,ARG111,VAL112,ARG139,HIS155,ALA158	57.7	69.8
26	VAL75,GLN76,PRO77,VAL82,VAL125, LEU126,VAL127	53.3	42
27	GLN197,LEU200,ALA205,ILE208	78.2	64.1
28	PHE7,ILE47,PRO52,ALA53,ASN54,ASN96,VAL98,ASP119	79.7	7.7
29	GLN45,THR48,GLY49,ASP50,ASN51,ASN256	90.6	68.9
30	LEU15,GLU19,ARG235,PRO246,GLN247	67	74.7
31	PRO193,ALA194,GLN197,ILE210	81.5	134
32	SER31,SER32,THR35,GLY62,ALA63,ALA109	106.8	101.3
33	LEU105,ASP106,VAL107,GLY108	130.2	255.6

The constructed model was corroborated by VERIFY 3D (Eisenberg *et al.,* 1997) to estimate the correctness of the model. The z-scores obtained from ProSA analysis for the modelled structures of CdtB protein found to be -5.15.

From the modelled structure using SPDBV program (Guex & Peitsch 1997) residues of 33 pockets for ligands interaction in the CdtB protein are shown in Fig. 3.

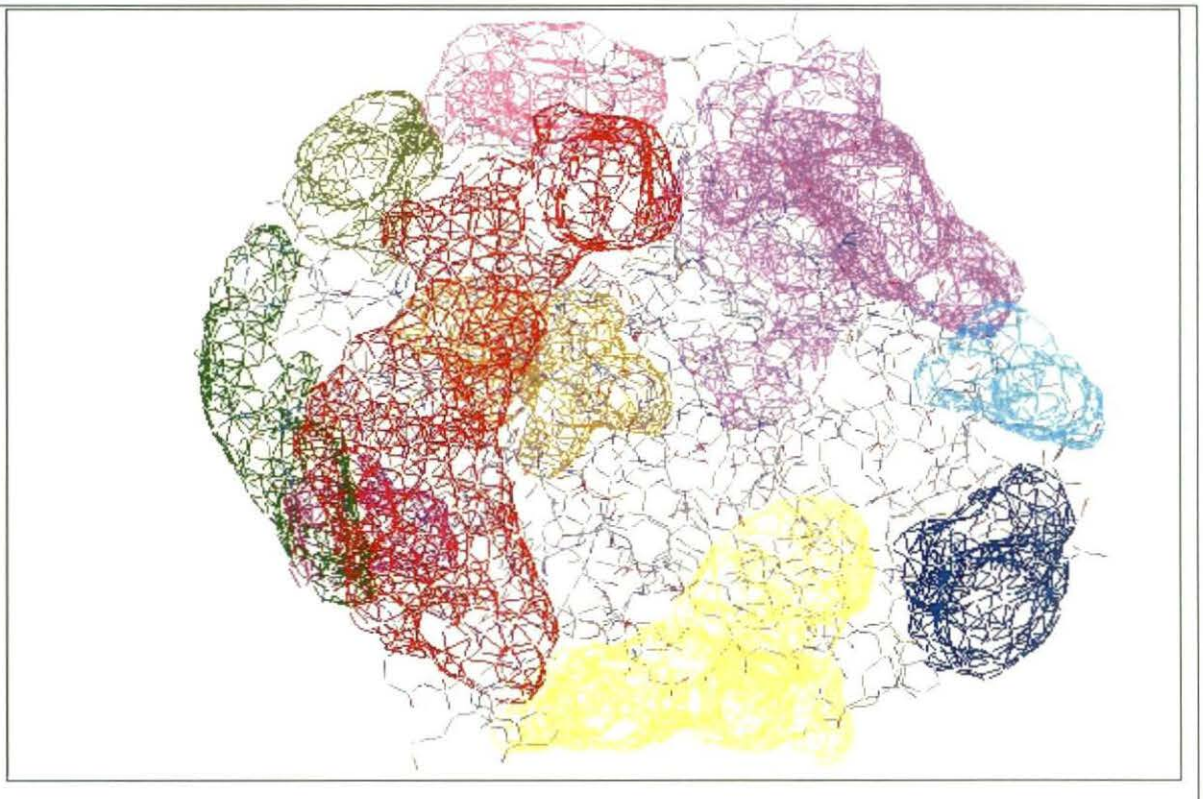

Figure-4: **Clefts and cavities**: Total 10 clefts and cavities in the surface of the protein are predicted using profunc server.

The refined model was submitted to ProFunc (http://www.ebi.ac.uk/thronton-srv/databases/ProFunc) (Laskowski *et al.,* 2005) to analyze the binding sites, showed the presence of 10 clefts and cavities in the surface of the protein shown in Fig. 4.

Nest analysis of the CdtB protein revealed the presence of six nests in this chain. It is found that when modelled CtdB protein from *H.Hepaticus* is compared with different enzyme templets it matches with two Dnase (PDB entry code 1dnk & 2dnj).

The Ramachandran plots (Ramachandran et al., 1963; Rajesh et al., 2007) illustrating the backbone conformation for the modelled protein is presented in Fig. 5.

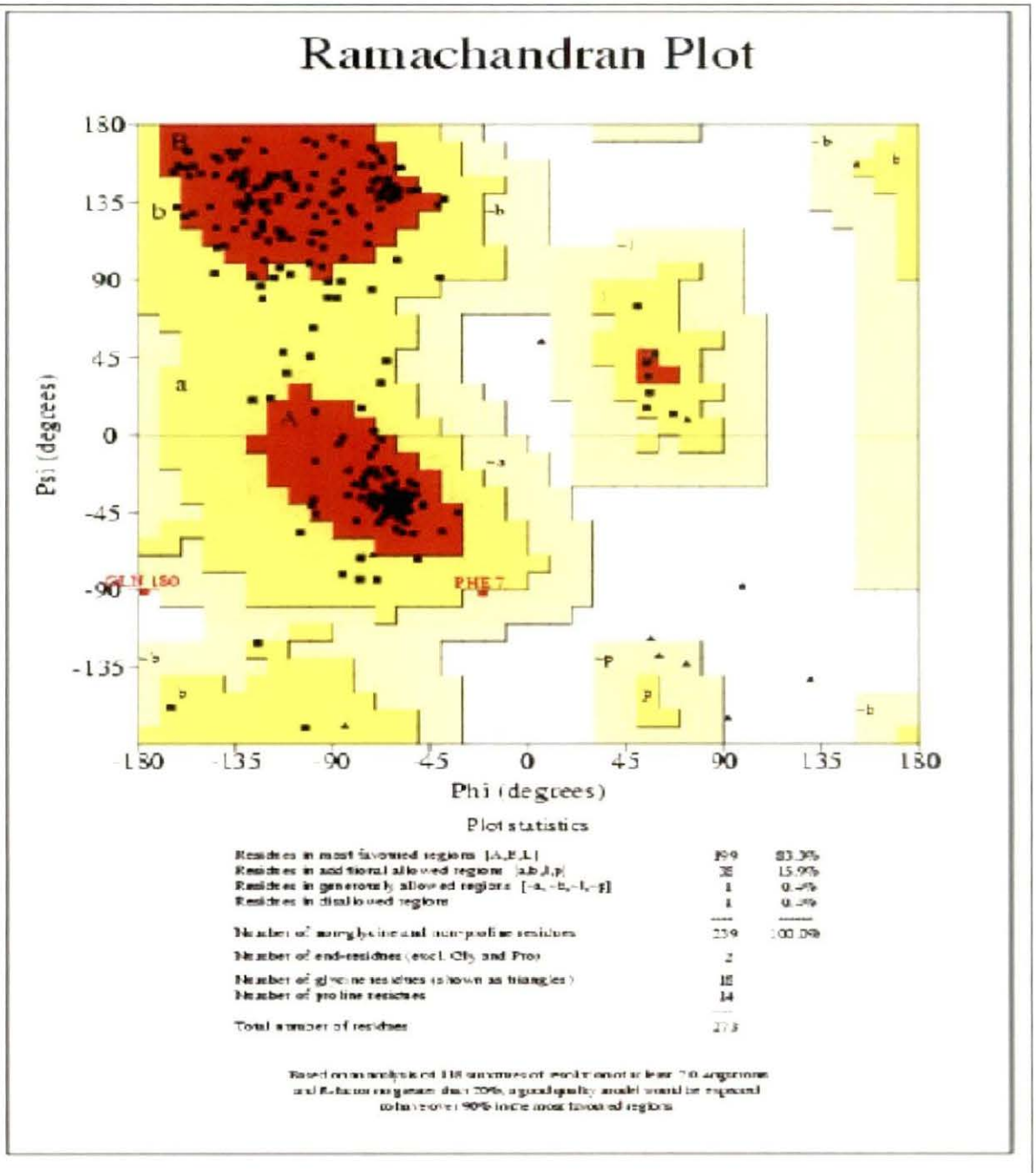

Figure-5: **Ramachandran plot:** Ramachandran plot of the CdtB proteins from *H. hepaticus* ATCC51449 shows the residue backbone conformations for the modelled CdtB protein.

PROCHECK analysis on the stereochemical quality of the 3D model structure of the modelled CdtB protein revealed that 83.3% of residues are in the most favored region in the Ramachandran plot. Moreover, the percentages of residues in the additional allowed regions

and generously allowed regions are 15.9% and 0.4%, respectively. However, 0.4% of residues remain on the disallowed region,

Molecular surface and electrostatic potential of modelled CdtB was generated using AutoDock Tools version 1.5.2 revision 2 (Goodshell *et al.*, 1996) and is presented in Fig. 6.

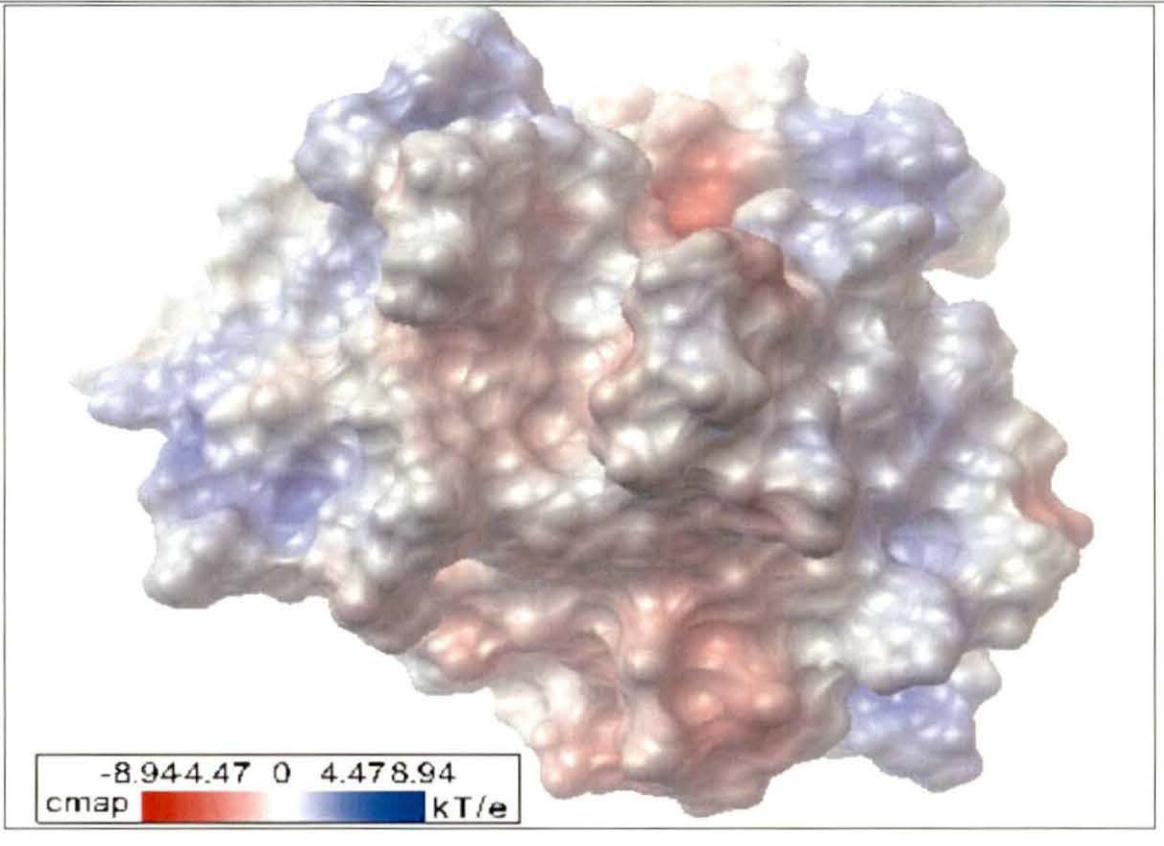

Figure-6: **Electrostatic surfaces:** Electrostatic surfaces of modeled protein CdtB from *H. hepaticus* ATCC51449 was calculated, which positive potential charges in blue, negative values in red and intermediate values in white by using AutoDock tools

Molecular dynamics simulation:

Molecular dynamics simulation of the modelled CdtB is performed and the resulting trajectory is analyzed to study the motional properties of the modelled protein CdtB. The time evolution of root mean square deviation (RMSD) is computed taking the modelled structure (CdtB) of the whole Protein as initial structure and presented in Fig. 7.

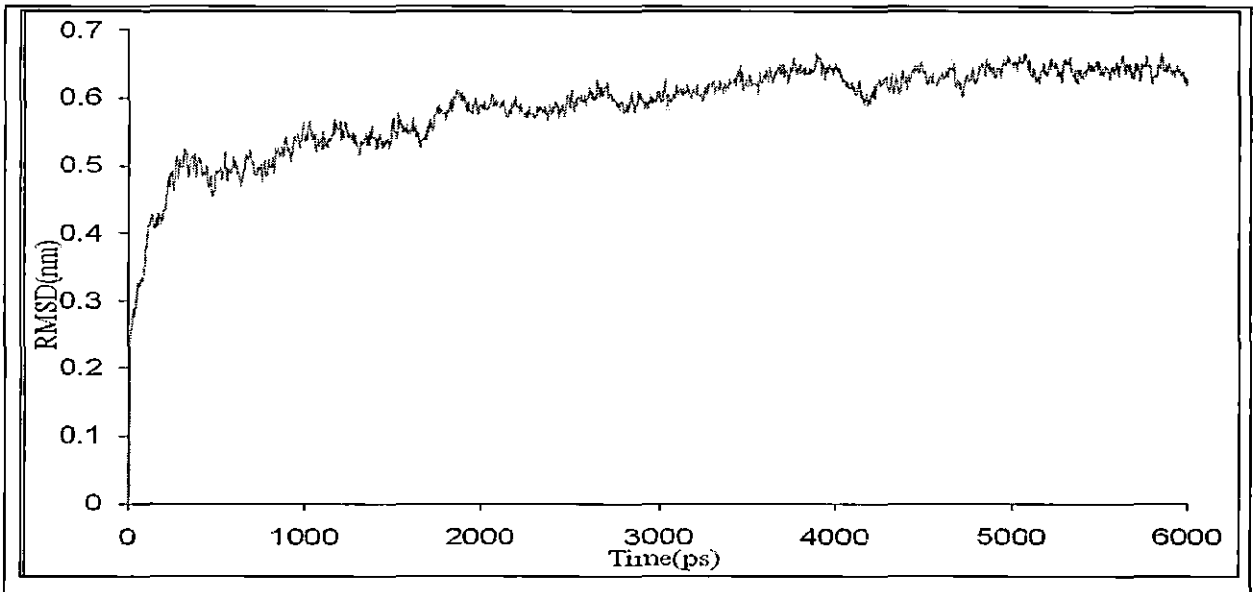

Figure-7: **RMSD:** Root mean square deviations (RMSD) of the CdtB proteins from *H. hepaticus* ATCC51449 protein as a function of time with respect to modeled protein was starting structure during the MD simulations

The time evolution of radius of gyration (Rg) is presented in Fig. 8.

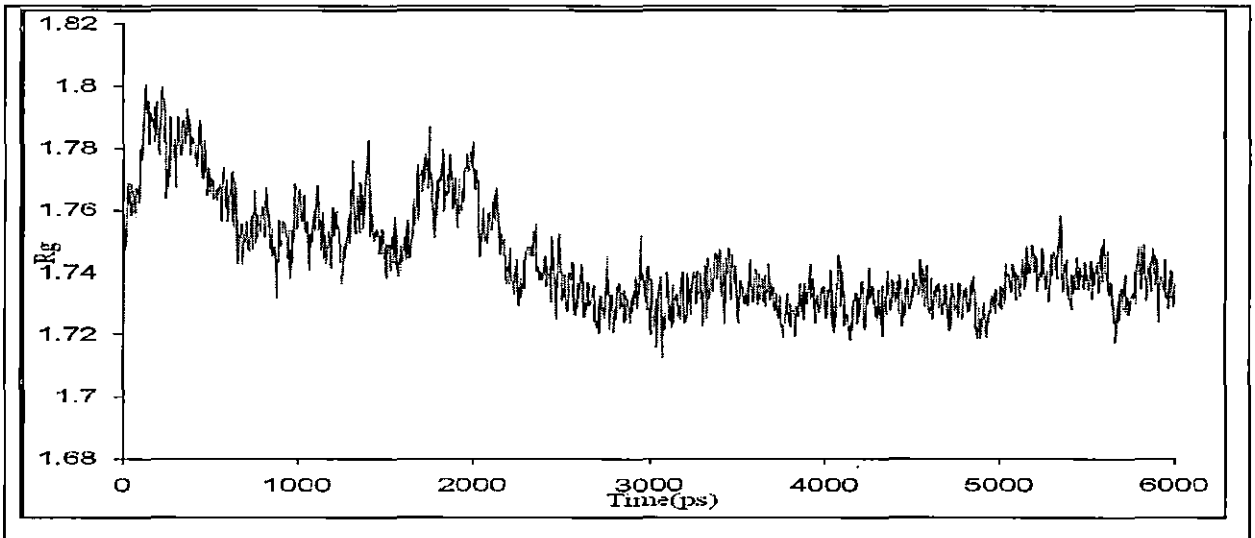

Figure-8: **Radius of gyration**: Radius of gyration (Rg) as a function of time with respect to starting structure during the MD simulations are shown for modelled CdtB protein from *H. hepaticus* ATCC51449

RMSF indicates the flexibility of the protein. RMSF of Cα is presented as a function of residue numbers in Fig. 9.

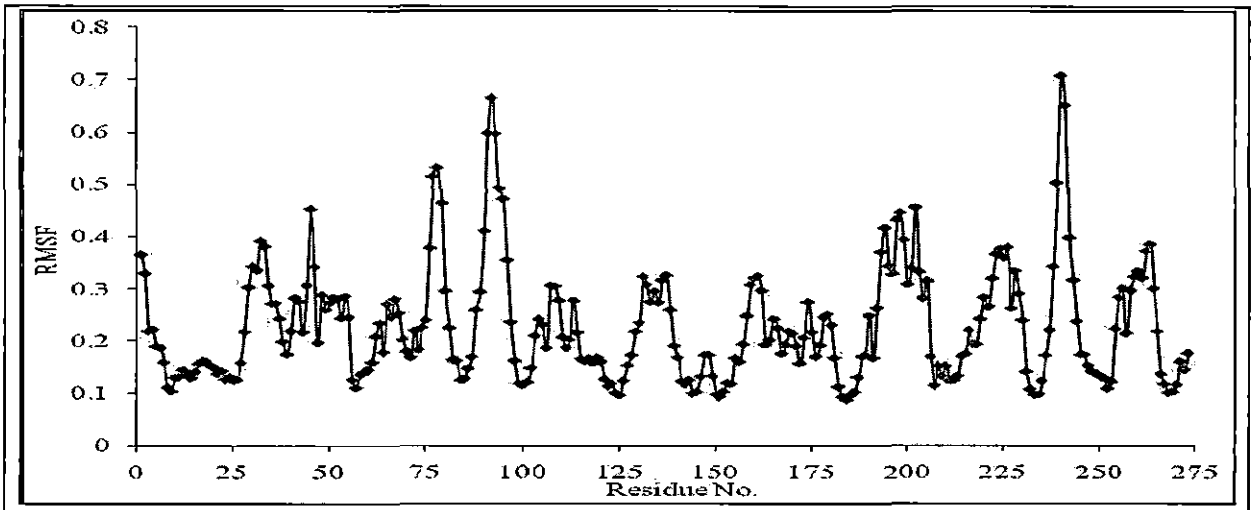

Figure-9: **Fluctuations:** Root means squared fluctuations (RMSF) of the Cα atoms during the MD simulations are shown for modelled CdtB protein of *H. hepaticus* ATCC51449

It is found that the number of hydrogen bonds ranged from 133 to 196 (Fig. 10) during the simulation.

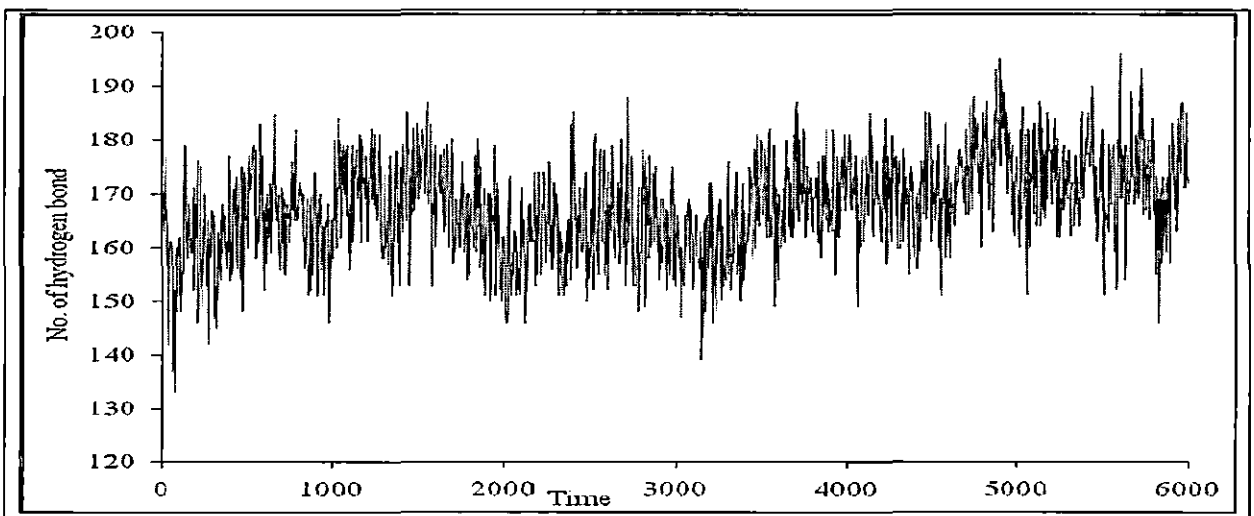

Figure-10: **Hydrogen Bond:** Number of Hydrogen Bonds during the whole Simulation time for modelled CdtB proteins of *Helicobacter hepaticus* ATCC51449

Principal component analysis (PCA): In order to further explore the nature of the fluctuations, principal component analysis (PCA) is carried out for the modelled protein CdtB (Amadei et al., 1993; Garcia 1992; Das & Mukhopadhyay 2007). It is seen that for the toxin 76.12 % fluctuations are captured by first 10 eigenvectors and the first eigenvector corresponds to 40.05 % of the total motion and the second 14.73% and third to a further 5.68 %.

The first four eigenvectors with largest eigenvalues were selected as the four principal components PC1, PC2, PC3 and PC4. Time evolution of principal component 1 (PC1), principal component 2 (PC2), principal component 3 (PC3) and principal component 4 (PC4) in water is represented in Fig. 11.

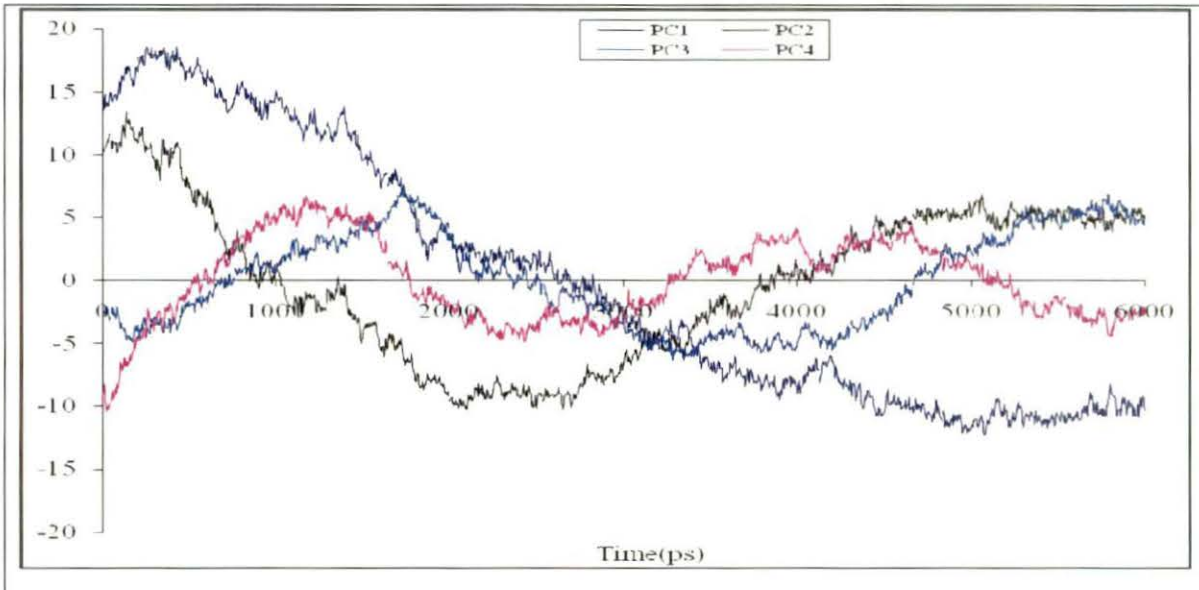

Figure-11: **Time evolution of PC**: Variation of four principle components with simulation time for modelled CdtB protein of *H. hepaticus* ATCC51449

The RMSF of Cα atoms calculated after projecting trajectories along their respective four principal components are presented in Fig. 12. It is evident from the analysis for CdtB that fluctuation is highest in the projection on PC1.

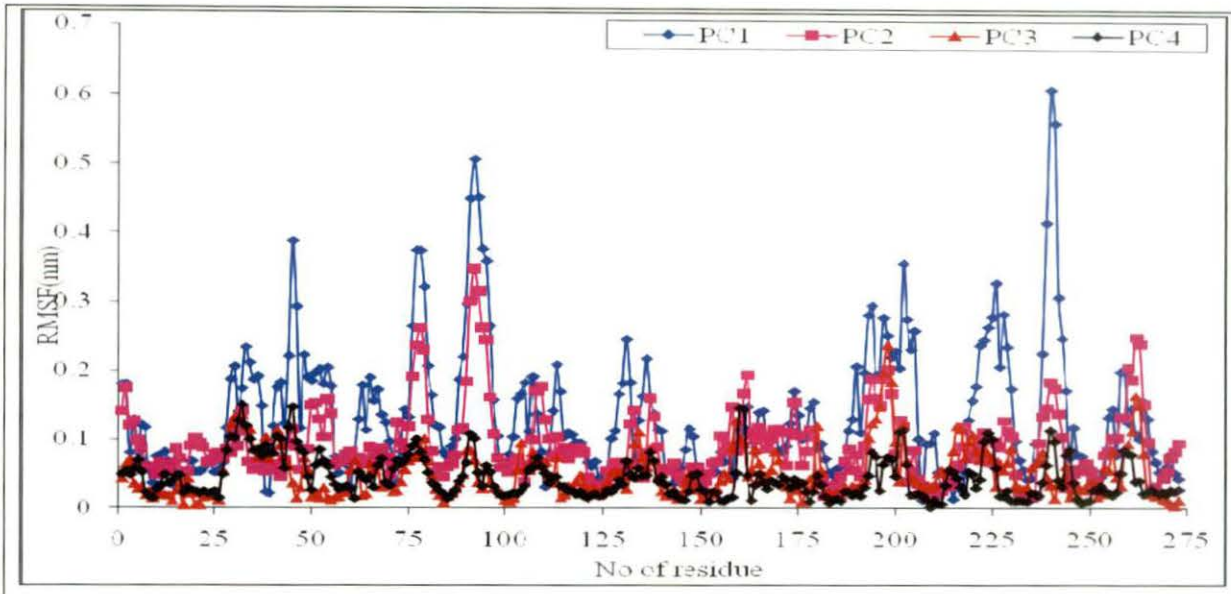

Figure-12: **Projections on PC**: The RMSF of Cα atoms calculated after projecting trajectories along their respective PC1, PC2, PC3 and PC4 directions for the modelled CdtB proteins of *H. hepaticus* ATCC51449

The probability of sampling the phase space determined by the first two principal modes during the simulations of the toxin is presented in Fig. 13.

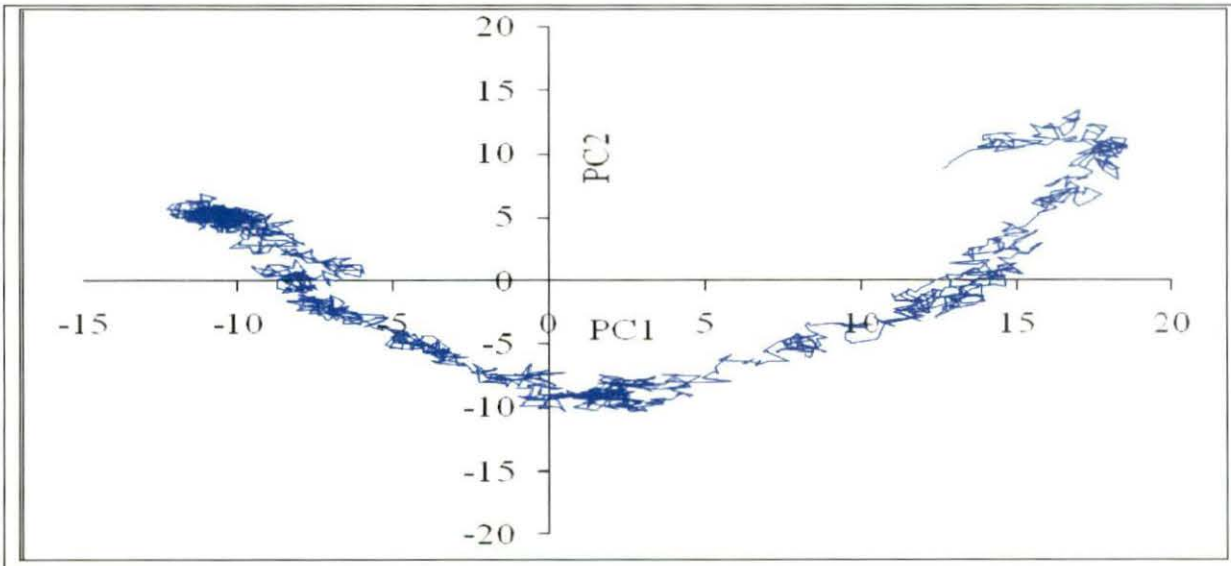

Figure-13: **Conformational Sampling**: The probability of sampling the phase space determined by principal modes 1 and 2 during the simulations of the modelled CdtB protein of *H. hepaticus* ATCC51449.

4. Discussions:

The modelled structures of the CdtB protein from *H. hepaticus* ATCC51449 shows that the helix and sheets remain interspersed throughout the protein structure (Fig. 2). VERIFY 3D revealed that 96.72% of the residues had an average 3D-1D score > 0.2.

Results of z scores from ProSA analysis specify that the z score of our model is very much within the range of scores normally found for proteins of comparable size. The value of the z-scores signifies that the 3D model of the CdtB protein is reliable and precise.

It is evident from Ramachandran plot (Fig. 5) that our predicted model protein CdtB carrying characteristics of a good quality of a model protein

Study of the molecular surface and electrostatic potential of modelled CdtB shows charged and polar residues are mostly on the surface. (Fig. 6).

It is evident from Fig.-7 that RMSD increased slowly up to 3,900 ps, and then decreases upto 4200ps then again slightly increases upto 5000ps. It is also clear from Rg, which shows a little variation upto 3000ps and after that almost attains equilibrium (Fig. 8). The RMSD and Rg calculations of CdtB suggest that the protein is less flexible in nature.

From RMSF, it is evident that the first and last residue fluctuates considerably. Interestingly, pronounced fluctuations are observed along some amino acid stretches (43-47, 75-81, 236-244,), which indicate the flexibility of the toxin in that region (Fig. 9).

The number of hydrogen bonds ranges from 133 to 196 (Fig. 10) revealed the fact that during the simulation, several hydrogen bonds broke and formed.

It is seen from Fig. 11 that time evolution of principal component 1 (PC1), principal component 2 (PC2), fluctuates remarkably in comparison to principal component 3 (PC3) and principal component 4 (PC4)

It is evident from the RMSF of Cα atoms calculated after projecting trajectories along their respective four principal components analysis for CdtB, fluctuation is highest in the projection on PC1 which indicates that PC1will provide more information regarding the collective motion of the protein (Fig. 12).

It is clear from the probability of sampling the phase space determined by first two principal modes during the simulations the projection of the dynamics trajectory onto the first two PC that the protein A traverse one conformational space around the origin and second one at the right side of the origin and third one at the left side of the origin which are much scattered indicating slightly high conformational freedom (Fig. 13)

The aim of our study was to construct three-dimensional model of the CdtB protein from *H. hepaticus* ATCC51449 using the homology modelling technique. The structures presented here are reliable on their biochemical features. The model may help to explain the functional mechanism of the Cdtb protein from *H. hepaticus* ATCC51449. The RMSD and Rg study explain the rigidity of toxin. This model is expected to assist the scientists working with the *H. hepaticus* ATCC51449 to recognize structure-function relationships of the CdtB protein. In absence of crystallographic or NMR structure this model will enlighten us about three dimensional structure and dynamic properties of the toxin CdtB and opening newer possibilities for exploring the molecular mechanism and activity in CdtB protein *H. hepaticus* ATCC51449.

8.5: References:

Altschul SF, Madden TL & Schaffer AA (1997) Gapped BLAST and PSI-BLAST: a new generation of protein database search programs. *Nucleic Acids Research,* **25**:3389-3402

Amadei A, Linssen ABM & Berendsen HJC (1993) Essential dynamics of proteins. *Proteins,* **17**:412–425

Avenaud P, Castroviejo M, Claret S, Rosenbaum J, Mégraud F & Ménard A (2004) Expression and activity of the cytolethal distending toxin of *Helicobacter hepaticus*. *Biochemical and Biophysical Research Communications* **318:**739–745

Berendsen HJC, Postma JPM, van Gusteren WF, Di Nola A & Haak JR (1984) Molecular dynamics with coupling to an external bath. *J. Chem. Phys.*, **81**:3684–3690

Bouzari S & Varghese A (1990) Cytolethal distending toxin (CLDT) production by enteropathogenic *Escherichia coli* (EPEC). *FEMS Microbiol. Lett.*, **59:**193–198

Centeno NB, Planas-Iglesias J & Oliva B (2005) Comparative modelling of protein structure and its impact on microbial cell factories. *Microbial Cell Factories.*, **4**:20 Doi: 10.1186/1475-2859-4-20

Cope L, Lumbley S, Latimer J, Klesney-Tait J, Stevens M, Johnson L, Purven M, Munson RJ, Lagergard T, Radolf J & Hansen E (1997) A diffusible cytotoxin of *Haemophilus ducreyi. Proc. Natl. Acad. Sci. USA.*, **94:**4056–4061

Darden T, York D & Pedersen L (1993) Particle mesh Ewald—an N.log (N) method for Ewald sums in large systems. *J. Chem. Phys.*, **98**:10089–10092

Das A & Mukhopadhyay C (2007) Application of principal component analysis in protein unfolding: An all-atom molecular dynamics simulation study. *The Journal of Chemical Physics,* **127**:165103-165108.

Dassanayake RP, Griep MA & Duhamel GE (2005) The cytolethal distending toxin B subunit of *Helicobacter hepaticus* is a Ca2+- and Mg2+-dependent neutral nuclease. *FEMS Microbiology Letters* **251**: 219–225.

Deng K & Hansen EJ (2003) A CdtA–CdtC complex can block killing of HeLa cells by *Haemophilus ducreyi* cytolethal distending toxin. *Infect. Immun.,* **71**: 6633–6640

Dlakic M (2000) Functionally unrelated signalling proteins contain a fold similar to Mg2þ-dependent endonucleases. *Trends Biochem. Sci.* **25**:272–273.

Dlakic M (2001) Is CdtB a nuclease or a phosphatase? *Science* **291**:547.

Dundas J, Ouyang Z, Tseng J, Binkowski A, Turpaz Y & Liang J (2006) CASTp: computed atlas of surface topography of proteins with structural and topographical mapping of functionally annotated residues. *Nucleic Acids Research*, **34**:116-118.

Eisenberg D, Luthy R & Bowie JU (1997) VERIFY3D: Assessment of protein models with three-dimensional profiles. *Methods in Enzymology,* **277**:396-404.

Elwell C, Chao K Patelet K & Dreyfus L (2001) *Escherichia coli* CdtB mediates cytolethal distending toxin cell cycle arrest, *Infect. Immun.,* **69**:3418–3422.

Elwell CA & Dreyfus LA (2000) DNase I homologous residues in CdtB are critical for cytolethal distending toxin-mediated cell cycle arrest. *Mol. Microbiol.* **37:** 952–963.

Essmann U, Perera L, Berkowitz ML, Darden T, Lee H & Pedersen LG (1995) A smooth particle mesh Ewald method. *J. Chem. Phys.,* **103**:8577–8593

Frisan T, Cortes-Bratti X, Chaves-Olarte E, Stenerlöw B & Thelestam M (2003). The *Haemophilus ducreyi* cytolethal distending toxin induces DNA double strand breaks and promotes ATM-dependent activation of RhoA. *Cell. Micro.,* **5**:695-707

Garcia AE (1992) Large-amplitude nonlinear motions in proteins. *Phys. Rev. Lett.,* **68**:2696–2699

Goodshell DS, Morris GM & Olson AJ (1996) Automated docking of flexible ligands: Applications of autodock, *Journal of Molecular Recognition*, **9**:1-5

Guex N & Peitsch, MC (1997) SWISS-MODEL and the Swiss-PdbViewer: An environment for comparative protein modeling. *Electrophoresis*, **18**:2714-2723

Hassane, DC, Lee RB, Mendenhall MD & Pickett CL (2001) Cytolethal distending toxin demonstrates genotoxic activity in a yeast model. *Infect. Immun* , **69**:5752.

Hess B, Bekker H, Berendsen HJC & Fraaije JGE (1997) LINCS: A linear constraint solver for molecular simulations. *Journal of Computational Chemistry* **18**:1463-1472.

Johnson WM & Lior H (1988) A new heat-labile cytolethal distending toxin (CLDT) produced by *Campylobacter* spp. *Microb. Pathog.,* **4**:115–126

Johnson WM & Lior H (1988b) A new heat-labile cytolethal distending toxin (CLDT) produced by *Escherichia coli* isolates from clinical material. *Microb. Pathog.,* **4**:103–113.

Lara-Tejero M & Galan JE (2002) Cytolethal distending toxin: limited damage as a strategy to modulate cellular functions. *Trends Microbiol.*, **10**:147–152.

Lara-Tejero M & Gala'n JE (2000) A bacterial toxin that controls cell cycle progression as a deoxyribonuclease I-like protein. *Science,* **290**: 354–357

Lara-Tejero M & Gala'n JE (2001) CdtA, CdtB, and CdtC form a tripartite complex that is required for cytolethal distending toxin activity. *Infect. Immun.*, **69**: 4358–4365

Laskowski RA, MacArthur MW, Moss DS & Thornton JM (1993) *PROCHECK*: a program to check the stereochemical quality of protein structures. *J. Appl. Cryst.*, **26**: 283-291

Laskowski RA, Watson JD & Thornton JM (2005) ProFunc: a server for predicting protein function from structure. *Nucleic Acids Research,* **33**:89-93.

Lee RB, Hassane DC, Cottle DL & Pickett CL (2003) Interactions of *Campylobacter jejuni* cytolethal distending toxin subunits CdtA and CdtC with HeLa cells. *Infect. Immun.*, **71**: 4883–4890

Lindahl E, Hess B & van der Spoel D (2001) GROMACS 3.0: a package for molecular simulation and trajectory analysis. *J. Mol. Modeling* **7**:306-317.

Mayer MPA, Bueno LC, Hansen EJ & DiRienzo JM (1999) Identification of a cytolethal distending toxin gene locus and features of a virulence-associated region in Actinobacillus actinomycetemcomitans. *Infect Immun.*, **67**:1227–1237.

Okuda J, Kurazono H & Takeda Y (1995). Distribution of the cytolethal distending toxin A gene (cdtA) among species of Shigella and Vibrio, and cloning and sequencing of the cdt gene from Shigella dysenteriae. *Microb. Pathog.*, **18**:167–172

Pickett CL & Whitehouse CA (1999) The cytolethal distending toxin family. *Trends. Microbiol.*, 7:292–297.

Pickett CL, Pesky EC, Cottle DL, Russell G, Erdem AN & Zeytin H (1996) Prevalence of cytolethal distending toxin production in *Campylobacter jejuni* and relatedness of Campylobacter sp. cdtB gene. *Infect. Immun.*, **64**:2070–2078

Rajesh R, Gunasekaran K, Muthukumaravel S, Balaraman K & Jambulingam P (2007) In Silico analysis of voltage-gated sodium channel in relation to DDT resistance in vector mosquitoes. *InSilico Biology,* 7:413-421.

Ramachandran GN, Ramakrishnan C & Sasisekharan V (1963) Stereochemistry of polypeptide chain configurations. *Journal of Molecular Biology*, 7:95-99.

Saiki K, Gomi T & Konishi K (2004) Deletion and purification studies to elucidate the structure of the *Actinobacillus actinomycetemcomitans* cytolethal distending toxin. *J. Biochem. (Tokyo),* **136**: 335–342

Saiki K, Konishi K, Gomi T, Nishihara T & Yoshikawa M (2001). Reconstitution and purification of cytolethal distending toxin of *Actinobacillus actinomycetemcomitans*. *Microbiol. Immunol.*, **45**: 497–506.

Sali A & Blundell TL (1993) Comparative protein modelling by satisfaction of spatial restraints. *Journal of Molecular Biology,* **234**:283-291.

Shenker BJ, Besack D, *McKay T, Pankoski L, Zekavat A & Donald R. Demuth DR* (2004) *Actinobacillus actinomycetemcomitans* cytolethal distending toxin (Cdt): Evidence that the holotoxin is composed of three subunits: CdtA, CdtB, and CdtC. *J. Immunol.*, **172:** 410–417

Suerbaum S, Josenhans C, Sterzenbach T, Drescher B, Brandt P, Bell M, Droge M, Fartmann B, Fischer HP, Ge Z, Hörster A, Holland *R,* Klein K, König J, Macko L, . Mendz GL, Nyakatura G, Schauer DB, Shen Z, Weber J, Frosch M & , Fox JG (2003) The complete genome sequence of the carcinogenic bacterium *Helicobacter hepaticus*. *PNAS.*, **100**:7901–7906

Sugai M, Kawamoto T, Peres SY, Ueno Y, Komatsuzawa H, Fujiwara T, Kurihara H, Suginaka H & Oswald E (1998) The cell cycle-specific growth-inhibitory factor produced by *Actinobacillus actinomycetemcomitans* is a cytolethal distending toxin. *Infect. Immun.*, **66:**5008–5019

Thompson JD, Higgins DG & Gibson TJ (1994) CLUSTAL W: improving the sensitivity of progressive multiple sequence alignment through sequence weighting, position-specific gap penalties and weight matrix choice. *Nucleic Acids Research,* **22**:4673-4680.

Ward JM, Fox JG, Anver MR, Haines DC, George CV Collins Jr. MJ, Gorelick PL, Nagashima K, gonad MA, gilden RV, Tully JG, Russell R, Benvensite RE, Paster BJ, Dewhirst, FE, Donovan JC, Anderson LM & rice JM (1994) Chronic active

hepatitis and associated liver tumors in mice caused by a persistent bacterial infection with a novel *Helicobacter* species. *J. Natl. Cancer Inst.*, **86**:1222–1227

Wiederstein M & Sippl M J (2007) ProSA-web: interactive web service for the recognition of errors in three-dimensional structures of proteins. *Nucleic Acids Research,* **35**: 407-410.

Yamada T, Komoto J, Saiki K, Konishi K & Takusagawa F (2006) Variation of loop sequence alters stability of cytolethal distending toxin (CDT): Crystal structure of CDT from *Actinobacillus actinomycetemcomitans. Protein Science.*, **15**:362–372

Yang LW, Rader AJ, Liu X, Jursa CJ, Chen SC, Karimi HA & Bahar I (2006) oGNM: A protein dynamics online calculation engine using the Gaussian Network Model. NucleicAcids Res., **34**:W24–31.

Young VB, Knox KA & Schaue DB (2000) Cytolethal distending toxin sequence and activity in the enterohepatic pathogen *Helicobacter hepaticus. Infect. Immun.*, **68**: 184–191.